Available online at www.sciencedirect.com
ScienceDirect
Trans. Nonferrous Met. Soc. China 25(2015) 1831−1839
Transactions of Nonferrous Metals Society of China
www.tnmsc.cn

Dynamic recrystallization mechanisms during hot compression of Mg−Gd−Y−Nd−Zr alloy

Yi-ping WU[1,2], Xin-ming ZHANG[1,2], Yun-lai DENG[1,2], Chang-ping TANG[1,2], Liu YANG[1,2], Ying-ying ZHONG[3]

1. School of Materials Science and Engineering, Central South University, Changsha 410083, China;
2. Key Laboratory of Nonferrous Metal Materials Science and Engineering, Ministry of Education, Central South University, Changsha 410083, China;
3. Defense Technology Research and Technology Center, China Aerospace Science and Industry Corporation, Beijing 100854, China

Received 25 July 2014; accepted 17 November 2014

Abstract: Hot compression tests were conducted on a homogenized Mg−7Gd−4Y−1Nd−0.5Zr alloy at 450 °C and a strain rate of 2 s^{-1}. Dynamic recrystallization (DRX) mechanisms were investigated by optical microscope (OM), scanning electron microscope (SEM) and transmission electron microscope (TEM) systematically. The crystallographic orientation information is obtained through electron back-scattering diffraction (EBSD). The result shows that the flow stress firstly reaches a peak rapidly followed by declining to a valley, and then increases gradually again when the alloy is compressed to a strain of −1.88. DRX related to $\{10\bar{1}2\}$ tensile twins is extensively observed at small strains, resulting in an evident grain refinement. DRX grains first nucleate along the edges of twin boundaries with about 30° $\langle 0001\rangle$ off the twin parents. While at large strains, conventional continuous DRX (CDRX) is frequently identified by the formation of small DRX grains along the original grain boundaries and the continuously increasing misorientation from the centre of large original grains to the grain boundaries. Evidence of particle-stimulated nucleation (PSN) is also observed in the present alloy.

Key words: Mg−RE alloy; hot compression; twin; dynamic recrystallization mechanism

1 Introduction

Magnesium (Mg) alloys show great potential for aircraft, automotive industry, 3C products and so on due to their low density and high specific strength [1]. For Mg alloys with hexagonal close-packed (HCP) structure, only two independent basal slip systems $(0002)\langle 11\bar{2}0\rangle$ are stimulated when deformed at room temperature, unable to accommodate the strain along *c*-axis. Twinning plays an important role in performing the *c*-axis strain and modifying the orientation, enabling the continuous deformation process [2,3]. With increasing temperatures, the workability of Mg alloys gradually increases as additional slip systems, such as prismatic slip and pyramidal slip, become available due to the decrease of the critical resolved shear stress. Meantime, during hot working, Mg alloys are liable to undergo dynamic recrystallization (DRX) because of the lower stacking fault energy. As both an improvement of formability and a modification of microstructure by refining grains, DRX has attracted a large amount of focus. DRX mechanisms can be generally classified into continuous DRX (CDRX) and discontinuous DRX (DDRX). CDRX is a recovery process characterized by continuous absorption of dislocations by subgrain boundaries, resulting in the high angle grain boundaries (HAGBs) to form new grains [4,5]. DDRX is a classic nucleation and growth process driven by the stored strain energy, operated by HAGBs migration [6]. In addition, various reported mechanisms were related to the deformation of Mg alloys, such as DRX grains nucleated along grain boundaries [7] and deformation bands [8], DRX related to deformation twins (TDRX) [9] and particle-stimulated nucleation (PSN) [10].

Recently, Mg−RE alloys have attracted a lot of interests due to the excellent mechanical properties at high temperatures by forming heat-resistant RE-rich

Corresponding author: Yun-lai DENG; Tel/Fax: +86-731-88830265; E-mail: luckdeng@csu.edu.cn
DOI: 10.1016/S1003-6326(15)63789-X

particles [11−13]. However, the authors collected a large number of publications regarding to DRX mechanisms in Mg alloys [14−16] but found that few work has yet been done to investigate DRX mechanisms of Mg−RE alloys. Although twinning behavior was frequently investigated in Mg alloys [17,18], most studies have focused on the twinning orientation at small strains or low strain rates [19−22]. How twinning behaves and its influence on microstructure evolution at high strain rates is rarely studied. Therefore, in this work, Mg−7Gd−4Y−1Nd−0.5Zr alloy is selected to execute hot compression deformation at a high strain rate of 2 s^{-1} to examine DRX mechanisms systematically. Twining behavior is also discussed in details during deformation. The deformation temperature is determined as 450 °C, under which the RE-rich particles are retained.

2 Experimental

Specimens for hot compression with dimensions of 25 mm × 20 mm × 10 mm were cut from an as-cast Mg−7Gd−4Y−1Nd−0.5Zr (mass fraction, %) ingot, and then homogenized at 520 °C for 10 h with subsequent cooling in air. The average grain size of the homogenized specimen is about 116 μm. Hot compression tests were carried out at 450 °C and a strain rate of 2 s^{-1} on a Gleeble−1500 test machine equipped with an automatic data acquisition system. The maximum true strain was −1.88. The interface between the specimen and the crosshead was lubricated with graphite to reduce friction, and thermocouple was welded on each specimen to record the real-time temperature during compression. Each specimen was heated up to the deformation temperature in 1 min and held isothermally for 3 min at the early stage of compression, and immediately quenched in water to maintain the deformation microstructure after compression. Then post-deformed measurements were conducted on the mid-plane sections perpendicular to the compression direction (CD).

For microstructure observation on XJP−6A optical microscope (OM) and Quanta−200 scanning electron microscope (SEM), specimens were cold mounted, water ground, mechanically polished and then etched in solution of 30 mL tartaric acid and 100 mL H_2O for about 25 s. Foils in a shape of 3 mm in diameter and 100 μm in thickness for transmission electron microscope (TEM) observation were ground and thinned using a twin-jet technique in the electrolyte of 4% HNO_3 and 96% methanol solution at −30 °C with a current of 60 mA. TEM microstructure was obtained by using FEI Tecnai G^2 20 operated at 200 kV. Electron back-scattering diffraction (EBSD) measurements were carried out using a Sirion−200 SEM equipped with an electron backscatter diffraction analysis system (TSL).

3 Results

3.1 Flow curve

Figure 1 presents the flow curve of the alloy compressed to a strain of −1.88 at 450 °C and a strain rate of 2 s^{-1}. According to the variation of the flow stress in the curve, compression deformation can be divided into three stages. In stage I, the hardening rate exceeds the softening rate in a large degree, thus, the flow stress increases sharply with the strain till the peak stress σ_p=172 MPa at the corresponding strain ε_p=−0.23. The flow stress goes down fiercely with increasing strain in stage II, and reaches the valley σ_v=79 MPa at the corresponding strain ε_v=−0.75. The flow stress decreases due to the softening caused by DRX. Notably, the stress rises again with strain during stage III with a lower hardening rate compared with stage I.

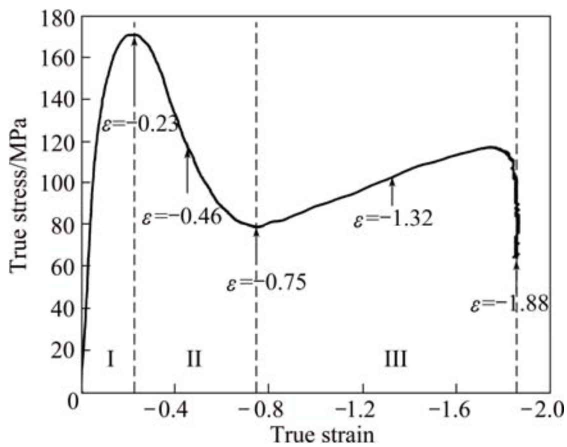

Fig. 1 Flow curve of alloy during compression at 450 °C and strain rate of 2 s^{-1}

3.2 Microstructural evolution

Figure 2 shows the optical microstructure of the alloy compressed to the corresponding strains as arrowed in Fig. 1. The microstructural evolution of the alloy with increasing strain is typical in HCP metals with the limited slip systems. At a small strain of −0.23, extensive twins are observed in some grains, as shown in Fig. 2(a). Also, attention should be paid to some original grain boundaries connected with twins. The boundaries become a bit curvy (as arrowed) in the presence of twins. There is no evident sign of DRX along grain boundaries. Figure 2(b) indicates that profuse twins induce DRX at a strain of −0.46. Besides parallel twins, there are some intersected ones. Consequently, the average grain size is largely reduced. And the original grain boundaries also shape with DRX grains (as arrowed). At a strain of −0.75 (Fig. 2(c)), more fine DRX grains along the original grain boundaries are formed and become to invade into the original grains. DRX grains firstly emerge at the

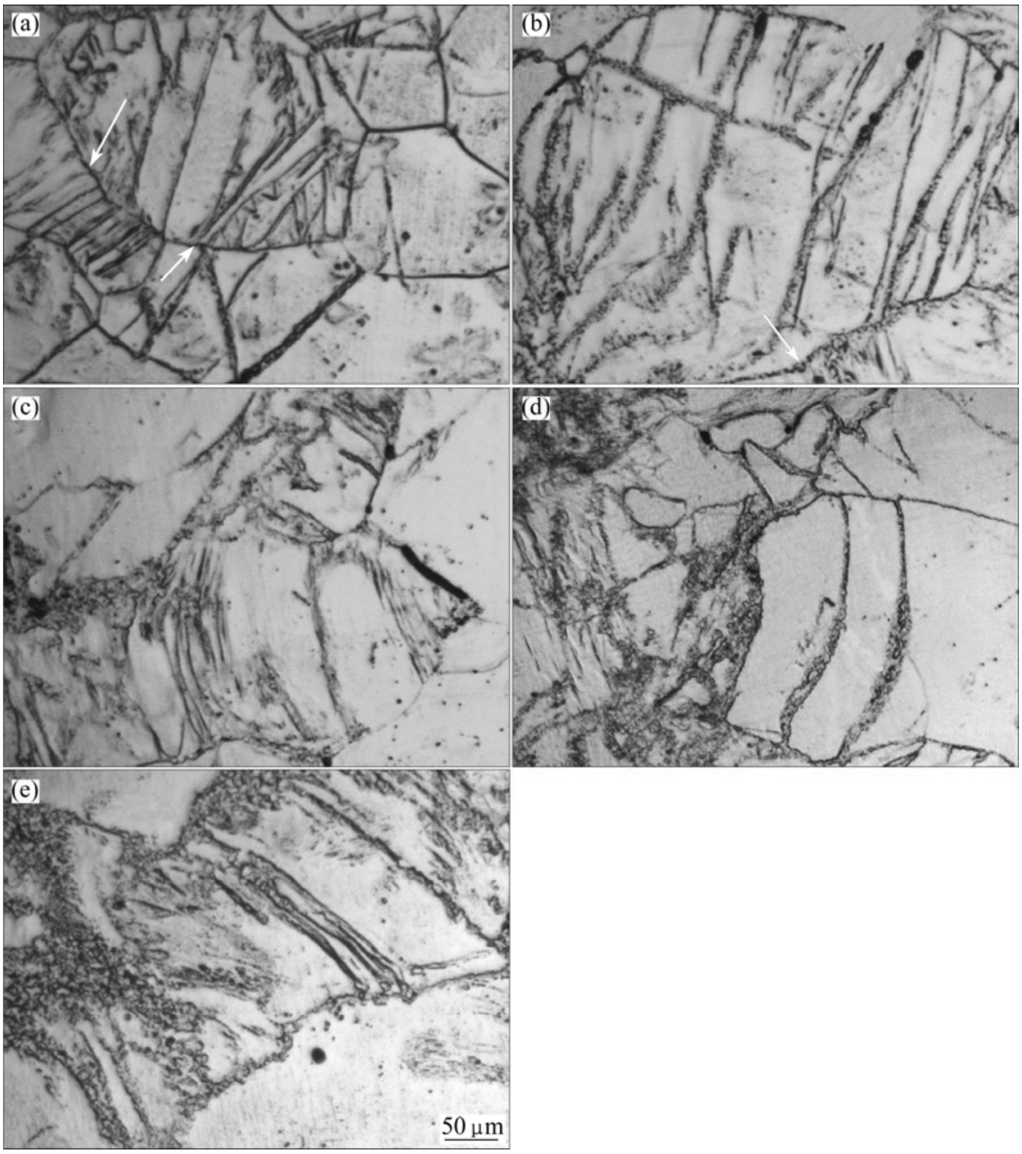

Fig. 2 Optical micrographs of alloy compressed to arrowed strains in Fig. 1: (a) ε=−0.23; (b) ε=−0.46; (c) ε=−0.75; (d) ε=−1.32; (e) ε=−1.88 (White arrows in Fig. 2(a) indicate curvy grain boundaries in the presence of twins; white arrow in Fig. 2(b) indicates original grain boundaries shaped with DRX grains)

grain boundary triple junctions, where the stored energy is relatively high. Figure 2(d) presents that some twins are widened by producing small DRX grains. What is more, the level of DRX is notably increased as the strain increases to −1.32. However, the DRX area fraction is much less than 100% even when the strain arrives at −1.88 (Fig. 2(e)). As seen, large non-recrystallized areas are still remained, resulting in the inhomogeneous microstructure. The flow stress increases firstly and decreases quickly mainly due to the large strain rate applied during compression. The microstructure is not fully recrystallized and is even influenced by twinning at the maximum strain of −1.88, which is different from the microstructural features observed in other similar alloys [23,24]. The microstructure was only characterized with DRX grains and unDRX coarse grains without any twins in the Mg−7Gd−5Y−1Nd−0.5Zr alloy compressed to a strain of −1.61 at 500 °C [23]. High density of deformation twins cut through the original grains with no signs of DRX in the Mg−8Gd−2Y−1Nd−0.3Zn−0.6Zr alloy compressed to −0.15 at 350 °C [24]. These two tests were both operated at a strain rate of 0.5 s^{-1}. Based on the above optical observation, the variation of flow stress is probably affected by DRX.

3.3 DRX mechanisms

3.3.1 TDRX

Figure 3 shows the EBSD result of the specimen strained to −0.46 under the optimal TDRX condition (Fig. 2(b)). The possible inducement to TDRX is that

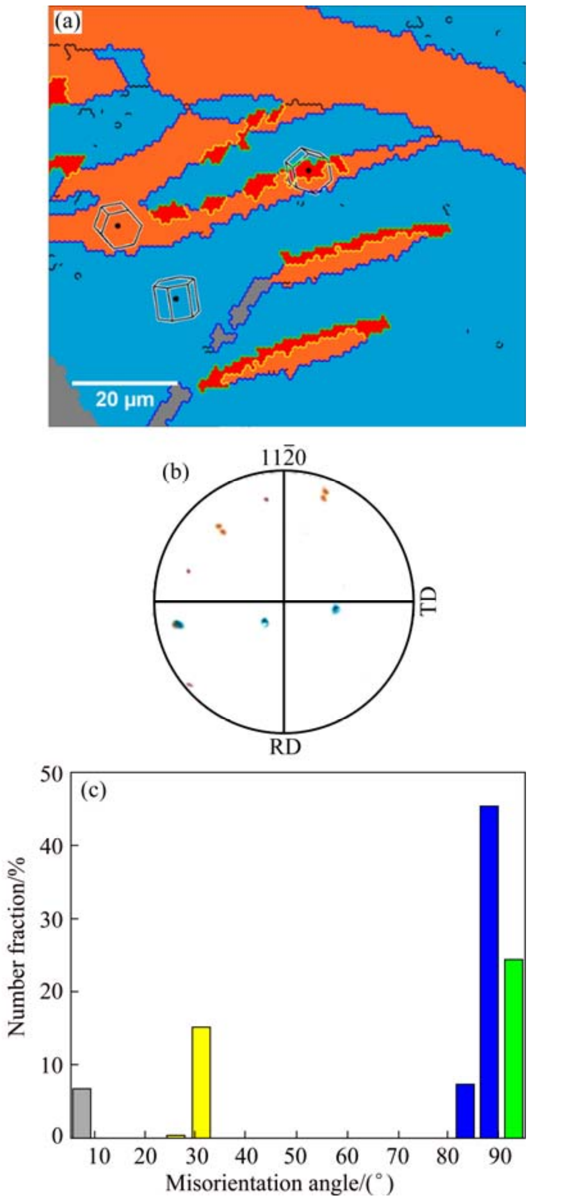

Fig. 3 EBSD results of alloy compressed to strain of −0.46: (a) Orientation image map (Three crystal cells indicate the orientations of the colored areas. The colored lines show the misorientation of boundaries which is further explained in Fig. 3(c)); (b) $(11\bar{2}0)$ pole figure (the colors of the points correspond to those of the areas in Fig. 3(a)); (c) Misorientation angle distribution (the colors of the bars correspond to those of the boundaries in Fig. 3(a))

twin boundaries act as barriers for dislocation motions so that dislocations concentrate inside twins, leading to a very high dislocation density. Twins store a lot of strain energy and provide the driving force for DRX. $\{10\bar{1}2\}$ tension twins can be easily activated when the *c*-axis is perpendicular to the compression stress, resulting in a basal plane tilt of 86.3° to the matrix [2]. In Fig. 3(a), tensile twins are confirmed by the misorientation of crystal cells marked in the blue area (the matrix) and the orange area (twins). Some twins are parallel to each other and become the nucleation sites of DRX. As seen, small DRX grains (red color) are located along the twin boundaries. The *c*-axes of DRX grains are rotated about 30° off the twins. This similar orientation relationship 30° ⟨0001⟩ between deformation and recrystallization texture was also reported in both processes of static recrystallization during annealing and DRX during hot plane strain compression of AZ31 alloy. It was ascribed to a discontinuous nucleation and growth process, not a recovery process like in-situ recrystallization or CDRX [25]. It was stated that this misorientation can only be attributed to DDRX because it necessitated grain boundary migration [26]. Tensile twins can be identified in the corresponding $(11\bar{2}0)$ pole figure (Fig. 3(b)). The misorientation angles of grain boundaries are shown in Fig. 3(c) where the misorientation between the twins and the matrix can also be determined.

Twinning is confirmed to be a very important deformation mechanism in the studied alloy because it not only induces DRX at small strains, such as −0.46, but also refines the grains at large strains. Figures 4(a) and (b) reveal TEM micrographs of the alloy compressed to a strain of −1.0. In Fig. 4(a), parallel twins segment the original grain, and twins further refine the grains by forming small DRX grains, as seen in Fig. 4(b). When the alloy was deformed to −1.45, it is clearly seen in Fig. 4(c) that small DRX grains first form along twin boundaries as the case observed in Fig. 3(a). The high density of dislocations inside twins will lead to the successive nucleation and growth of DRX grains upon further straining.

3.3.2 CDRX

TEM images in Fig. 5 show the evidence of CDRX when the alloy was compressed to a strain of −1.0. In Fig. 5(a), the motion of dislocations is blocked, and dislocations pile up in the vicinity of grain boundaries, resulting in the formation of dislocation network. In Fig. 5(b), dislocations interact with each other and tangle together to form dislocation cells. Dislocation cells are further converted to subgrains. Finally, subgrains grow to be small new DRX grains near grain boundaries, as shown in Fig. 5(c).

Moreover, CDRX can be identified by an increase in misorientation from the original grain centre to its grain boundary [27]. Figure 6(a) gives the misorientation angle map of grain boundaries obtained from EBSD when the alloy was compressed to a strain of −1.88. Thick black lines correspond to HAGBs (misorientation angle ≥15°), while low-angle boundaries are represented by thin black lines (misorientation angle ≥5°) and thin white lines (misorientation angle ≥2°). Subgrains decorated with thin black lines and thin white lines are located in both small DRX grains and large original

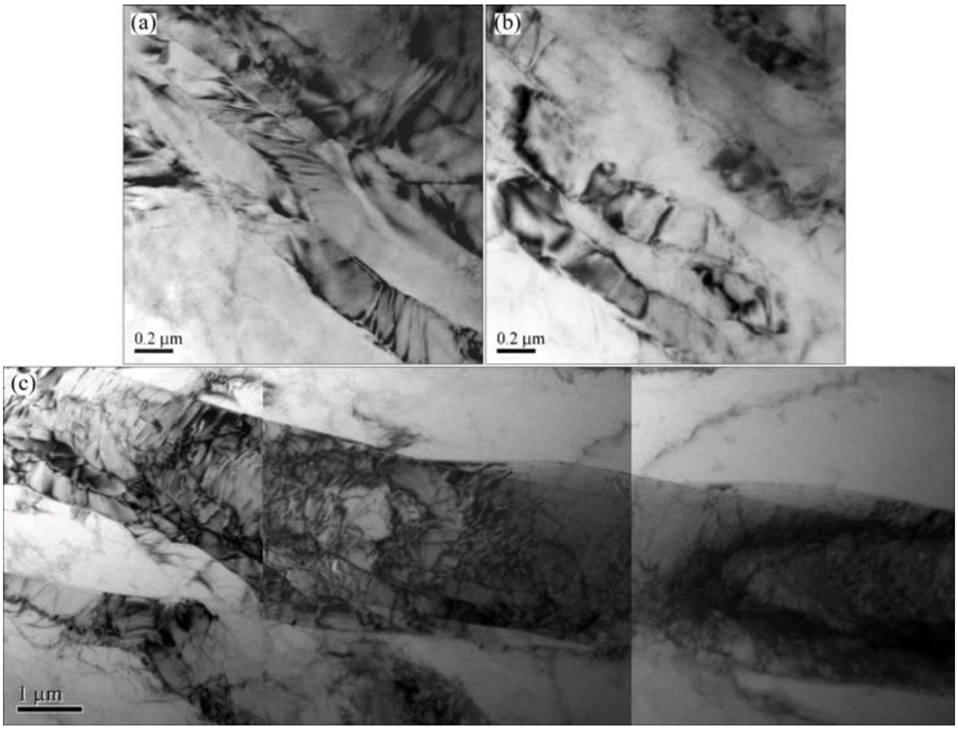

Fig. 4 TEM micrographs of alloy compressed to strain of −1.0 (a,b) and −1.45 (c)

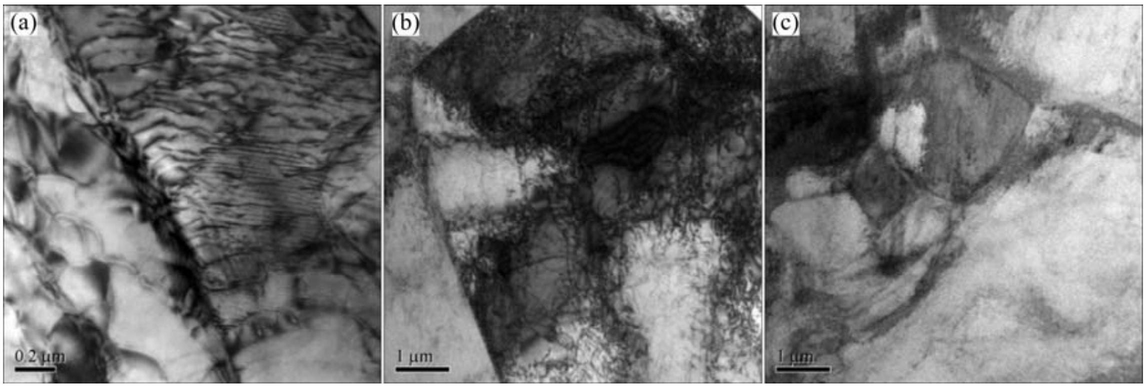

Fig. 5 TEM images of alloy compressed to strain of −1.0: (a) Grain boundaries blocking motion of dislocations; (b) Dislocation cells formed along grain boundaries; (c) Subgrains converting to small DRX grains

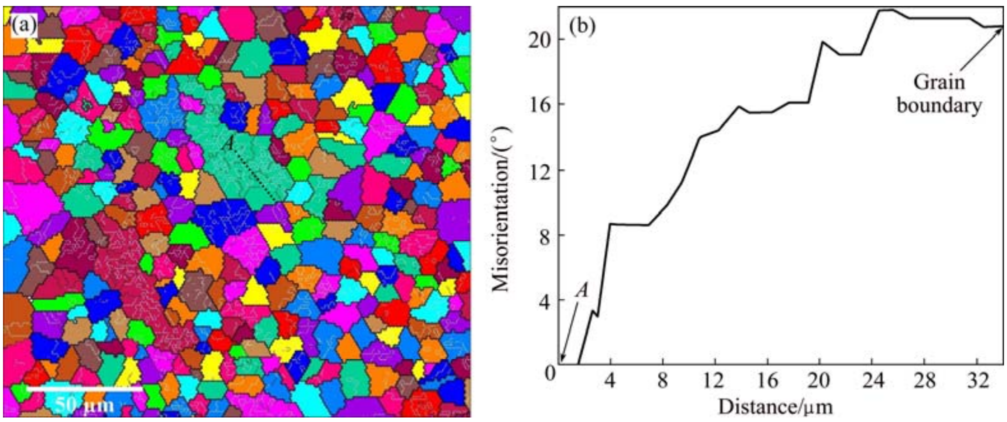

Fig. 6 (a) Grain boundary misorientation map of alloy compressed to strain of −1.88 (Thick black lines correspond to HAGBs (misorientation angle ≥15°), while low-angle boundaries are represented by thin black lines (misorientation angle ≥5°) and thin white lines (misorientation angle ≥ 2°)); (b) Evolution of accumulated misorientation along dotted line in selected grain in Fig. 6(a)

grains, particularly, thin black lines are more frequently seen in large grains. This observation is similar with what was observed in Al−5% Mg alloy [27], which exhibited a well-developed subgrain structure that extended further toward the grain interior. The point-to-origin misorientation along the dotted line from the interior point *A* to the grain boundary in one large grain shows that the maximum misorientation is greater than 20°, as shown in Fig. 6(b). The misorientation feature accords with the operation of CDRX in Mg alloys.

3.3.3 Particle-stimulated nucleation mechanism

Figure 7 shows how particles affect DRX behavior in the alloy deformed to a strain of −1.88. Figure 7(a) reveals that small DRX grains have developed in regions associated with particles. In other words, RE-rich particles are frequently observed in or near DRX grains. This may be ascribed to high contents of RE elements in the alloy. Figure 7(b) indicates that dislocations are pinned by some particles. Particles and dislocations interact during the continuous deformation. The movement of dislocations becomes more difficult due to the barriers brought by particles, forcing the dislocations to pile up, and tangle and form dislocation cells. High-density dislocation cells convert to subgrains, resulting in fine grains finally, which is known as PSN mechanism. PSN has been previously reported in Mg alloys [10,28], and it is expected to be very normal in Mg−RE alloys considering the precipitating behavior of RE elements.

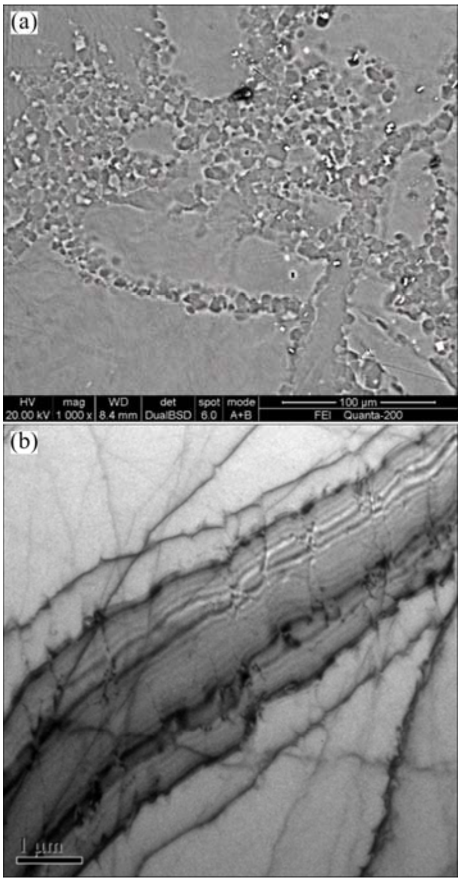

Fig. 7 SEM image (a) and TEM image (b) of alloy compressed to strain of −1.88

4 Discussion

4.1 Strain softening

Flow stress under the maximum strain of −1.88 at 450 °C and a strain rate of 2 s^{-1} (Fig. 1) renders the alloy undergoing DRX during compression: after initial work hardening, a peak stress is attained, followed by obvious work softening, and then the stress rises again with increasing strain because the hardening rate exceeds the softening rate. The similar charts of flow curve have been observed during compression tests at the lowest temperature or the highest strain rate in other Mg alloys [29,30]. During the compression test of AZ31 alloy at 200 °C and a strain rate of 0.01 s^{-1}, the sample underwent massive strain localization which resulted in failure by shearing once strained to −1.4. When examining the interior region of the fractured sample, a necklace-type DRX microstructure consisting of very fine DRX grains with an average grain size of 1−2 μm and unDRX original large grains was observed [29]. In this work, fine DRX grains with an average size of 6−7 μm are formed around large original grains in the alloy strained to −1.88 (Fig. 2(e) and Fig. 7(a)), while the difference is that twinning participates to induce DRX during the softening stage II (Fig. 2(b)).

Two reasons may contribute to the decrease of stress from the peak to the lowest value in stage II: Tensile twinning and DRX during hot deformation. Figure 8 shows the EBSD result of the alloy strained to −0.39. In Fig. 8(a), apparent parallel $\{10\bar{1}2\}$ tensile twins (red area) are observed in one coarse grain (blue area) without the sign of TDRX. Figures 8(b) and (c) show the corresponding (0001) pole figure and the misorientation angle map of grain boundaries, respectively. Usually, the homogenized alloy has grains with initial random crystallographic orientation [23]. In this work, the homogenized sample has coarse grains. It is expected that its initial texture is random and weak. Profuse tensile twins occur under the strain of −0.39. It was claimed that the flow softening at moderate strains during compression was due to the grain reorientations brought about by tensile twinning [19]. It was also stated that tensile twinning caused the reorientation of basal planes from a hard slip to a softer direction, enabling the continual plastic flow during longitudinal tensile deformation [3]. BARNETT [2] ascribed the increase in uniform elongation during tensile loading to the occurrence of tension twinning. Because of the extensive occurrence of tensile twins in stage II, it is probable that

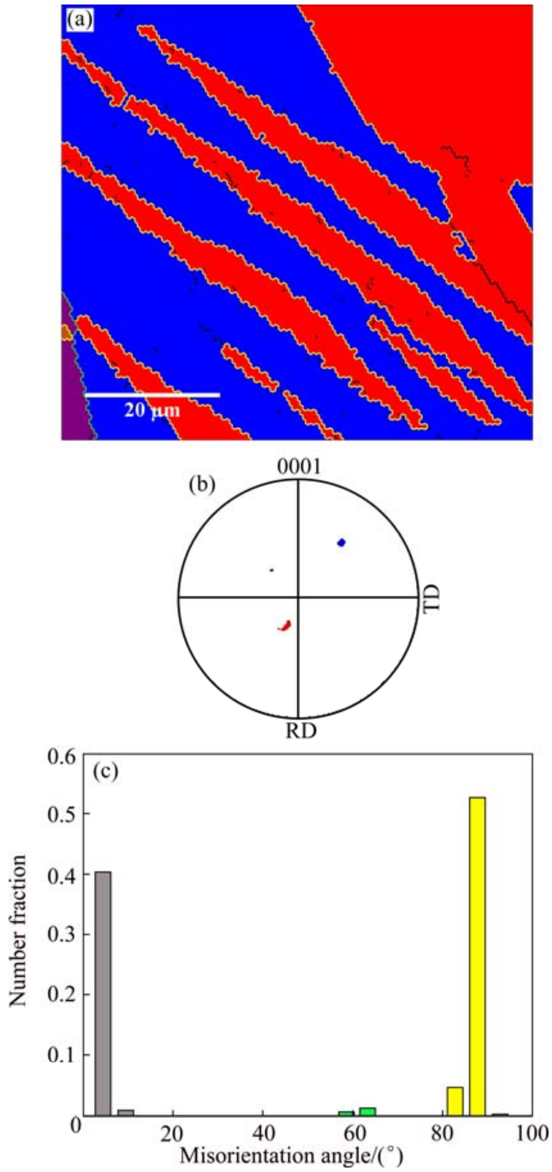

Fig. 8 EBSD result of alloy compressed to strain of −0.39: (a) Orientation image map (blue area is the matrix, red area is tensile twins, the colored lines show the misorientation of boundaries; (b) (0001) pole figure (the colors of the points correspond to those areas in Fig. 8(a)); (c) Misorientation angle distribution (the colors of the bars correspond to those boundaries in Fig. 8(a))

the texture is modified during deformation to ensure a larger deformation strain; It is well known that DRX is a restoration or softening mechanism which can reduce the dislocation density and release the accumulated energy to facilitate straining [31]. The profuse occurrence of TDRX and DRX along grain boundaries (Fig. 2(b)) contributes to the softening in stage II.

4.2 Twinning behavior

Interestingly, grain boundaries which have triggered twins tend to be curvy, as observed in Fig. 2(a). It is well understood that the nucleation centers for twinning are mainly defects in the crystal structure [32]. Some researchers suggested that twin nucleation most likely occurred at grain boundaries and twin nucleation strongly depended on structures of grain boundaries and the local stress state [33]. For tensile twins, studies showed that twin nuclei can locate at grain boundaries, dislocation pile-ups in the grain interior and particle surfaces. Particularly, grain boundaries with the misorientation angles between 10° and 35° were preferential places for tensile twin nucleation [34].

Recently, several publications claimed that there was a direct relationship between DRX mechanisms and deformation mechanisms in Mg alloys during thermo-mechanical processes [35,36]. During hot rolling of AZ31 alloy, $\{10\bar{1}1\}-\{10\bar{1}2\}$ double twin related DRX nucleation was mainly observed in the normal direction (ND) plate samples where dislocation glide was considered as the main deformation mechanism accompanied with double twins. Grain boundary related DRX nucleation was mainly observed in the transverse direction (TD) plate samples where $\{10\bar{1}2\}$ tensile twin was the dominant deformation mechanism. The differences of DRX mechanism in the ND and TD plate samples were caused by the different initial textures [35]. Both twin boundaries and grain boundaries become nucleation sites of DRX in the studied alloy due to the initial random texture (see Fig. 2(b)).

TDRX produces a misorientation component of 30° ⟨0001⟩ in this alloy (see Fig. 3), similar to the results observed after DDRX in AZ series alloys [25,26]. However, unlike AZ series alloys, TDRX is still observed at a large strain of −1.45 (see Fig. 4(c)) due to the feature of high temperature resistance of the studied alloy. Furthermore, the DRX area fraction is much less than 100% under the maximum strain of −1.88. This may be associated with a lack of further nucleation sites once the original grain boundaries have been completely decorated with DRX grains. It may also be related to strain localized in the DRX area during deformation because of the large difference in sizes of the initial grains and DRX grains [37,38].

5 Conclusions

1) Flow stress first climbs fast to a peak, and falls to the lowest, and rises again till the maximum strain of −1.88. The softening in stage II is attributed to DRX nucleated along grain boundaries and twin boundaries; while it may also be associated with the orientation change brought about by tensile twinning.

2) EBSD analysis shows that the misorientation between the $\{10\bar{1}2\}$ tensile twin and TDRX grain is 30° ⟨0001⟩. TEM images indicate that twins refine the

microstructure through segmenting the original grains and nucleating DRX grains first along twin boundaries. Increasing strain does not eliminate twinning to accommodate the deformation due to the high strain rate applied.

3) The evolution of DRX microstructure proceeds with the growth of dislocation cells to subgrains, and then to small DRX grains along original grain boundaries. Grain boundary misorientation map from EBSD data further confirms the occurrence of continuous DRX (CDRX) at high strains. Particle-stimulated nucleation (PSN) appears to be another DRX mechanism in this alloy.

References

[1] LUO A A. Recent magnesium alloy development for elevated temperature applications [J]. International Materials Reviews, 2004, 49(1): 13−30.

[2] BARNETT M R. Twinning and the ductility of magnesium alloys: Part I: Tension twins [J]. Materials Science and Engineering A, 2007, 464(1−2): 1−7.

[3] SUH B C, SHIM M S, KIM D W, KIM N J. Twinning behavior of Mg−4Zn−1Gd alloy sheet during longitudinal tensile deformation [J]. Scripta Materialia, 2013, 69(6): 465−468.

[4] YAN H, XU S W, CHEN R S, KAMADO S, HONMA T, HAN E H. Twins, shear bands and recrystallization of a Mg−2.0%Zn−0.8%Gd alloy during rolling [J]. Scripta Materialia, 2011, 64(2): 141−144.

[5] YANG Xu-yue, JI Ze-sheng, MIURA H, SAKAI T. Dynamic recrystallization and texture development during hot deformation of magnesium alloy AZ31 [J]. Transactions of Nonferrous Metals Society of China, 2009, 19(1): 55−60.

[6] MA Ming-long, ZHANG Kui, LI Xing-gang, LI Yong-jun, ZHANG Kang. Hot deformation behavior of rare earth magnesium alloy without pre-homogenization treatment [J]. Transactions of Nonferrous Metals Society of China, 2008, 18(S1): s132−s139.

[7] GALIYEV A, KAIBYSHEV R, GOTTSTEIN G. Correlation of plastic deformation and dynamic recrystallization in magnesium alloy ZK60 [J]. Acta Materialia, 2001, 49(7): 1199−1207.

[8] LI Li. Deformation band and texture of a cast Mg−RE alloy under uniaxial hot compression [J]. Materials Science and Engineering A, 2011, 528(24): 7178−7185.

[9] MA Q, LI B, MARIN E B, HORSTEMEYER S J. Twinning-induced dynamic recrystallization in a magnesium alloy extruded at 450 °C [J]. Scripta Materialia, 2011, 65(9): 823−826.

[10] AL-SAMMAN T. Modification of texture and microstructure of magnesium alloy extrusions by particle-stimulated recrystallization [J]. Materials Science and Engineering A, 2013, 560: 561−566.

[11] HE S M, ZENG X Q, PENG L M, GAO X, NIE J F, DING W J. Microstructure and strengthening mechanism of high strength Mg−10Gd−2Y−0.5 Zr alloy [J]. Journal of Alloys and Compounds, 2007, 427(1): 316−323.

[12] ZHANG Xin-ming, LI Li, DENG Yun-lai, ZHOU Nan. Superplasticity and microstructure in Mg−Gd−Y−Zr alloy prepared by extrusion [J]. Journal of Alloys and Compounds, 2009, 481(1−2): 296−300.

[13] ZHANG Xin-ming, TANG Chang-ping, DENG Yun-lai, YANG Liu, LIU Wen-jun. Phase transformation in Mg−8Gd−4Y−Nd−Zr alloy [J]. Journal of Alloys and Compounds, 2011, 509(21): 6170−6174.

[14] YANG Xu-yue, MIURA H, SAKAI T. Dynamic evolution of new grains in magnesium alloy AZ31 during hot deformation [J]. Materials Transactions, 2003, 44(1): 197−203.

[15] LIU Zhi-yi, BAI Song, KANG S B. Low-temperature dynamic recrystallization occurring at a high deformation temperature during hot compression of twin-roll-cast Mg−5.51Zn−0.49Zr alloy [J]. Scripta Materialia, 2009, 60(6): 403−406.

[16] XU S W, KAMADO S, MATSUMOTO N, HONMA T, KOJIMA Y. Recrystallization mechanism of as-cast AZ91 magnesium alloy during hot compressive deformation [J]. Materials Science and Engineering A, 2009, 527(1−2): 52−60.

[17] BARNETT M R, KESHAVARZ Z, BEER A G, MA X. Non-Schmid behaviour during secondary twinning in a polycrystalline magnesium alloy [J]. Acta Materialia, 2008, 56(1): 5−15.

[18] BEYERLEIN I J, CAPOLUNGO L, MARSHALL P E, MCCABE R J, TOMÉ C N. Statistical analyses of deformation twinning in magnesium [J]. Philosophical Magazine, 2010, 90(16): 2161−2190.

[19] LIU X, JONAS J J, LI L X, ZHU B W. Flow softening, twinning and dynamic recrystallization in AZ31 magnesium [J]. Materials Science and Engineering A, 2013, 583: 242−253.

[20] BAJARGAN G, SINGH G, SIVAKUMAR D, RAMAMURTY U. Effect of temperature and strain rate on the deformation behavior and microstructure of a homogenized AZ31 magnesium alloy [J]. Materials Science and Engineering A, 2013, 579: 26−34.

[21] BARNETT M R, DAVIES C H J, MA X. An analytical constitutive law for twinning dominated flow in magnesium [J]. Scripta Materialia, 2005, 52(7): 627−632.

[22] YU Z Z, CHOO H. Influence of twinning on the grain refinement during high-temperature deformation in a magnesium alloy [J]. Scripta Materialia, 2011, 64(5): 434−437.

[23] XIA Xiang-sheng, ZHANG Kui, LI Xing-gang, MA Ming-long, LI Yong-jun. Microstructure and texture of coarse-grained Mg−Gd−Y−Nd−Zr alloy after hot compression [J]. Materials & Design, 2013, 44: 521−527.

[24] HOU Xiu-li, CAO Zhan-yi, SUN Xu, WANG Li-dong, WANG Li-min. Twinning and dynamic precipitation upon hot compression of a Mg−Gd−Y−Nd−Zr alloy [J]. Journal of Alloys and Compounds, 2012, 525: 103−109.

[25] GOTTSTEIN G, AL-SAMMAN T. Texture development in pure Mg and Mg alloy AZ31 [J]. Materials Science Forum, 2005, 495−497: 623−632.

[26] AL-SAMMAN T, LI X, CHOWDHURY S G. Orientation dependent slip and twinning during compression and tension of strongly textured magnesium AZ31 alloy [J]. Materials Science and Engineering A, 2010, 527(15): 3450−3463.

[27] HUMPHREYS F J, HATHERLY M. Recrystallization and related annealing phenomena [M]. Oxford: Elsevier, 2004: 427−444.

[28] ROBSON J D, HENRY D T, DAVIS B. Particle effects on recrystallization in magnesium-manganese alloys: Particle-stimulated nucleation [J]. Acta Materialia, 2009, 57(9): 2739−2747.

[29] AL-SAMMAN T, GOTTSTEIN G. Dynamic recrystallization during high temperature deformation of magnesium [J]. Materials Science and Engineering A, 2008, 490(1−2): 411−420.

[30] HELIS L, OKAYASU K, FUKUTOMI H. Microstructure evolution and texture development during high-temperature uniaxial compression of magnesium alloy AZ31 [J]. Materials Science and Engineering A, 2006, 430(1−2): 98−103.

[31] McQUEEN H J, IMBERT C A C. Dynamic recrystallization: Plasticity enhancing structural development [J]. Journal of Alloys and Compounds, 2004, 378(1−2): 35−43.

[32] CHRISTIAN J W, MAHAJAN S. Deformation twinning [J]. Progress in Materials Science, 1995, 39(1): 1−157.

[33] WANG J, BEYERLEIN I J, TOMÉ C N. An atomic and probabilistic perspective on twin nucleation in Mg [J]. Scripta Materialia, 2010, 63(7): 741−746.

[34] MOLNÁR P, JÄGER A, LEJČEK P. Twin nucleation at grain

boundaries in Mg−3wt.% Al−1wt.% Zn alloy processed by equal channel angular pressing [J]. Scripta Materialia, 2012, 67(5): 467−470.
[35] WANG Mao-yin, XIN Ren-long, WANG Bing-shu, LIU Qing. Effect of initial texture on dynamic recrystallization of AZ31 Mg alloy during hot rolling [J]. Materials Science and Engineering A, 2011, 528(6): 2941−2951.
[36] COTTAM R, ROBSON J, LORIMER G, DAVIS B. Dynamic recrystallization of Mg and Mg−Y alloys: Crystallographic texture development [J]. Materials Science and Engineering A, 2008, 485(1−2): 375−382.
[37] ION S E, HUMPHREYS F J, WHITE S H. Dynamic recrystallisation and the development of microstructure during the high temperature deformation of magnesium [J]. Acta Metallurgica, 1982, 30(10): 1909−1919.
[38] KAIBYSHEV R O, GALIEV A M, SOKOLOV B K. Effect of grain size on the plastic deformation and dynamic recrystallization of a magnesium alloy [[Previously Titled: Grain size effect on plastic deformation and dynamic recrystallization in magnesium alloy.]] [J]. Phys Met Metallogr, 1994, 78(2): 209−217. (in Russian)

Mg−Gd−Y−Nd−Zr 合金热压缩变形的动态再结晶机制

吴懿萍[1,2]，张新明[1,2]，邓运来[1,2]，唐昌平[1,2]，杨 柳[1,2]，仲莹莹[3]

1. 中南大学 材料科学与工程学院，长沙 410083；
2. 中南大学 有色金属材料科学与工程教育部重点实验室，长沙 410083；
3. 中国航天科工集团公司 防御技术研究试验中心，北京 100854

摘 要：在变形温度为 450 °C 和应变速率为 2 s^{-1} 的条件下对均匀化退火后的 Mg−7Gd−4Y−1Nd−0.5Zr 合金进行热压缩试验。采用金相显微镜(OM)、扫描电镜(SEM)和透射电镜(TEM)综合分析合金变形过程中的动态再结晶机制。采用电子背散射衍射(EBSD)获得晶体微取向信息。结果表明：随应变逐渐增加到−1.88，合金流变应力先快速升高到某个峰值，随后下降到最低值，最后又开始逐渐上升。在低应变下，大量 $\{10\bar{1}2\}$ 拉伸孪晶诱发形核形成动态再结晶晶粒，导致晶粒明显细化。动态再结晶晶粒首先在孪晶边界进行形核，且与孪晶母体存在 30° $\langle 0001\rangle$ 的取向差。在大应变下，合金组织中在原始大晶粒附近形成细小动态再结晶晶粒，且从原始大晶粒内部到其晶界处的累积微取向连续增加，从而确定合金发生了连续动态再结晶。合金中也发现了粒子激发形核的动态再结晶机制。

关键词：Mg−RE 合金；热压缩；孪晶；动态再结晶机制

(Edited by Yun-bin HE)